

# Mesenchymal stem cell-mediated reversal of bronchopulmonary dysplasia and associated pulmonary hypertension

Georg Hansmann<sup>1</sup>, Angeles Fernandez-Gonzalez<sup>1</sup>, Muhammad Aslam<sup>1</sup>, Sally H. Vitali<sup>2</sup>, Thomas Martin<sup>3</sup>, S. Alex Mitsialis<sup>1</sup>, and Stella Kourembanas<sup>1</sup>

<sup>1</sup>Department of Pediatrics, Division of Newborn Medicine, <sup>2</sup>Department of Anesthesia, <sup>3</sup>Department of Pediatrics, Division of Respiratory Diseases, Children's Hospital Boston, Harvard Medical School, Boston, Massachusetts, USA.

G.H. and A.F.G. contributed equally as first authors

## ABSTRACT

Clinical trials have failed to demonstrate an effective preventative or therapeutic strategy for bronchopulmonary dysplasia (BPD), a multifactorial chronic lung disease in preterm infants frequently complicated by pulmonary hypertension (PH). Mesenchymal stem cells (MSCs) and their secreted components have been shown to prevent BPD and pulmonary fibrosis in rodent models. We hypothesized that treatment with conditioned media (CM) from cultured mouse bone marrow-derived MSCs could reverse hyperoxia-induced BPD and PH. Newborn mice were exposed to hyperoxia (FiO<sub>2</sub>=0.75) for two weeks, were then treated with one intravenous dose of CM from either MSCs or primary mouse lung fibroblasts (MLFs), and placed in room air for two to four weeks. Histological analysis of lungs harvested at four weeks of age was performed to determine the degree of alveolar injury, blood vessel number, and vascular remodeling. At age six weeks, pulmonary artery pressure (PA acceleration time) and right ventricular hypertrophy (RVH; RV wall thickness) were assessed by echocardiography, and pulmonary function tests were conducted. When compared to MLF-CM, a single dose of MSC-CM-treatment (1) reversed the hyperoxia-induced parenchymal fibrosis and peripheral PA devascularization (pruning), (2) partially reversed alveolar injury, (3) normalized lung function (airway resistance, dynamic lung compliance), (4) fully reversed the moderate PH and RVH, and (5) attenuated peripheral PA muscularization associated with hyperoxia-induced BPD. Reversal of key features of hyperoxia-induced BPD and its long-term adverse effects on lung function can be achieved by a single intravenous dose of MSC-CM, thereby pointing toward a new therapeutic intervention for chronic lung diseases.

**Key Words:** airway hyperresponsiveness, chronic lung disease of infancy, lung vascular pruning, lung injury, hyperoxia


Bronchopulmonary dysplasia (BPD) is a complex chronic lung disease (CLD) with multifactorial etiology, characterized by the arrest of alveolar and vascular growth associated with inflammation and parenchymal fibrosis.<sup>[1-4]</sup> Historically, oxygen toxicity and ventilator-induced injury have been the prerequisites for BPD in premature infants born at less than 28-32 weeks gestation with respiratory distress syndrome, but BPD may also occur in immature infants with few signs of initial lung injury. Approximately one in four infants with moderate-to-severe BPD develops pulmonary hypertension (PH)<sup>[5]</sup> that can be triggered

by inflammation and endothelial dysfunction, and perpetuated through alveolar hypoxia. Importantly, the occurrence of PH in BPD is not only an epiphenomenon or minor secondary event, but appears to greatly increase mortality (estimated death rate is 47% two years after diagnosis of PH).<sup>[6]</sup> Moreover, with an increasing percentage of extremely immature newborns surviving in the post-surfactant era, BPD is one of the most common primary diagnoses in neonatal follow-up and pediatric

### Address correspondence to:

**Dr. Stella Kourembanas**  
Division of Newborn Medicine  
Children's Hospital Boston  
Harvard Medical School  
300 Longwood Avenue  
Boston, MA 02115, USA  
Email: stella.kourembanas@childrens.harvard.edu

### Access this article online

<b>Quick Response Code:</b>	<b>Website:</b> <a href="http://www.pulmonarycirculation.org">www.pulmonarycirculation.org</a>
	<b>DOI:</b> 10.4103/2045-8932.97603
	<b>How to cite this article:</b> Hansmann G, Fernandez-Gonzalez A, Aslam M, Vitali SH, Martin T, Mitsialis SA et al. Mesenchymal stem cell-mediated reversal of bronchopulmonary dysplasia and associated pulmonary hypertension. <i>Pulm Circ</i> 2012;2:170-81.

PH clinics today. Bronchopulmonary dysplasia as a major etiologic factor for PH development has been recognized and, in fact, BPD was assigned its own category in the recently published classification of pediatric pulmonary hypertensive vascular disease (PPHVD Category 4: BPD; PVRI Panama classification, 2011).<sup>[7]</sup>

The saccular stage of murine lung development is completed after two weeks of postnatal alveolarization. Hence, the developmental stage of the mouse lung at birth resembles that in the human preterm neonate between 24 and 28 weeks gestation, making the newborn mouse an excellent model to study human developmental lung injury. Hyperoxia-induced lung damage in neonatal mice is characterized by rarefaction and simplification of alveoli and thickened alveolar septa, inflammation and parenchymal fibrosis, a pattern which is similar to human BPD.<sup>[8]</sup>

Mesenchymal stem cells, also referred to as multipotent stromal cells (MSCs), have attracted significant attention as potential cell-based therapy for BPD and other severe lung diseases because these multipotent cells exhibit beneficial effects in related animal models through anti-inflammatory, immunomodulatory, pro-survival (endothelial, epithelial), and anti-fibrotic mechanisms.<sup>[9,10]</sup> We and others have previously shown that administration of bone marrow-derived MSCs prevent BPD/CLD of prematurity,<sup>[11,12]</sup> acute lung injury,<sup>[13,14]</sup> and pulmonary fibrosis<sup>[9]</sup> in experimental models despite low engraftment rates. Our previous study revealed that conditioned media (CM) from MSCs was most effective in preserving alveolar architecture in the hyperoxia-BPD mouse model and suggested that bone marrow-derived MSCs have important cytoprotective effects predominantly via paracrine mechanisms.<sup>[11]</sup>

Although innovative approaches for the prevention of mechanical ventilation, oxidative stress, and ultimately BPD have been developed recently,<sup>[15-17]</sup> larger studies have failed so far to demonstrate an efficient preventative or therapeutic strategy for BPD in preterm newborn infants.<sup>[18]</sup> From a clinical perspective, reversal rather than postnatal prevention of oxygen-induced lung injury such as BPD is most relevant, given that (1) BPD probably has prenatal origins (preeclampsia,<sup>[19,20]</sup> oligohydramnios,<sup>[5]</sup> chorioamnionitis<sup>[21,22]</sup>), and (2) hyperoxic lung injury occurs in the first few minutes and hours of life when endotracheal intubation, mechanical ventilation, and oxidative stress cannot be avoided due to respiratory failure.<sup>[15,23]</sup>

While the human umbilical cord or placenta may serve as a source for future clinical MSC applications,<sup>[24]</sup> we herein used CM from cultured mouse bone marrow-derived MSCs as a feasible intravenous treatment in

the well-established murine hyperoxia-BPD model. We found that several weeks after injury, MSC-CM-treatment (1) reversed the parenchymal fibrosis and peripheral pulmonary arterial devascularization (PA pruning), (2) partially reversed the alveolar injury, (3) normalized the airway hyperresponsiveness, (4) fully reversed the moderate PH and right ventricular hypertrophy (RVH), and (5) attenuated peripheral PA muscularization that was associated with BPD. Thus, hyperoxia-induced BPD and associated PH can be reversed with MSC-CM-treatment, thereby pointing toward a new therapeutic approach for chronic lung diseases with alveolar and vascular injury. Importantly, we show that a single intravenous dose of MSC-CM after the acute phase of lung injury in the neonatal period inhibits longterm impairment of lung function, an increasingly recognized serious complication of BPD.

## MATERIALS AND METHODS

### Experimental design

Mouse pups (FVB) were exposed to 75% oxygen from postnatal day 1 (P1) to P14 (Fig. 1, upper panel), or remained in room air from birth (normoxic controls). On P14, when chronic hyperoxic lung injury is evident in this BPD model,<sup>[8,11]</sup> the mice were placed in room air, and intravenously injected with concentrated MSC-CM containing 10 µg protein, or the equivalent amount of mouse lung fibroblast-CM (MLF-CM) as control. Two weeks after the end of hyperoxia, i.e., after two weeks recovery in room air at postnatal age four weeks, lung tissue was harvested for histology and immunohistochemistry as described below. Four weeks after the end of hyperoxia, i.e., at postnatal age six weeks and body weight of 18-22 grams, all mice (including normoxic controls) underwent echocardiography and pulmonary function tests. All animal experiments were approved by the Children's Hospital Boston Animal Care and Use Committee.

### Hyperoxia chamber

Neonatal pups were pooled and exposed to 75% oxygen in a plexiglass chamber or to room air beginning at birth and continuing for 14 days. Ventilation was adjusted by an Oxycycler controller (Biospherix, Lacona, N.Y.) to remove CO<sub>2</sub> so that it did not exceed 5,000 ppm (0.5%). Ammonia was removed by ventilation and activated charcoal filtration through an air purifier. Dams were rotated from hyperoxia to room air every 48 hours to prevent excessive oxygen toxicity to the adult mice.

### Cell isolation, culture, and differentiation

Bone marrow-derived MSCs were isolated from the femurs and tibiae of 5- to 7-week-old FVB mice as previously described.<sup>[11,25-27]</sup> Briefly, the bone marrow cells were

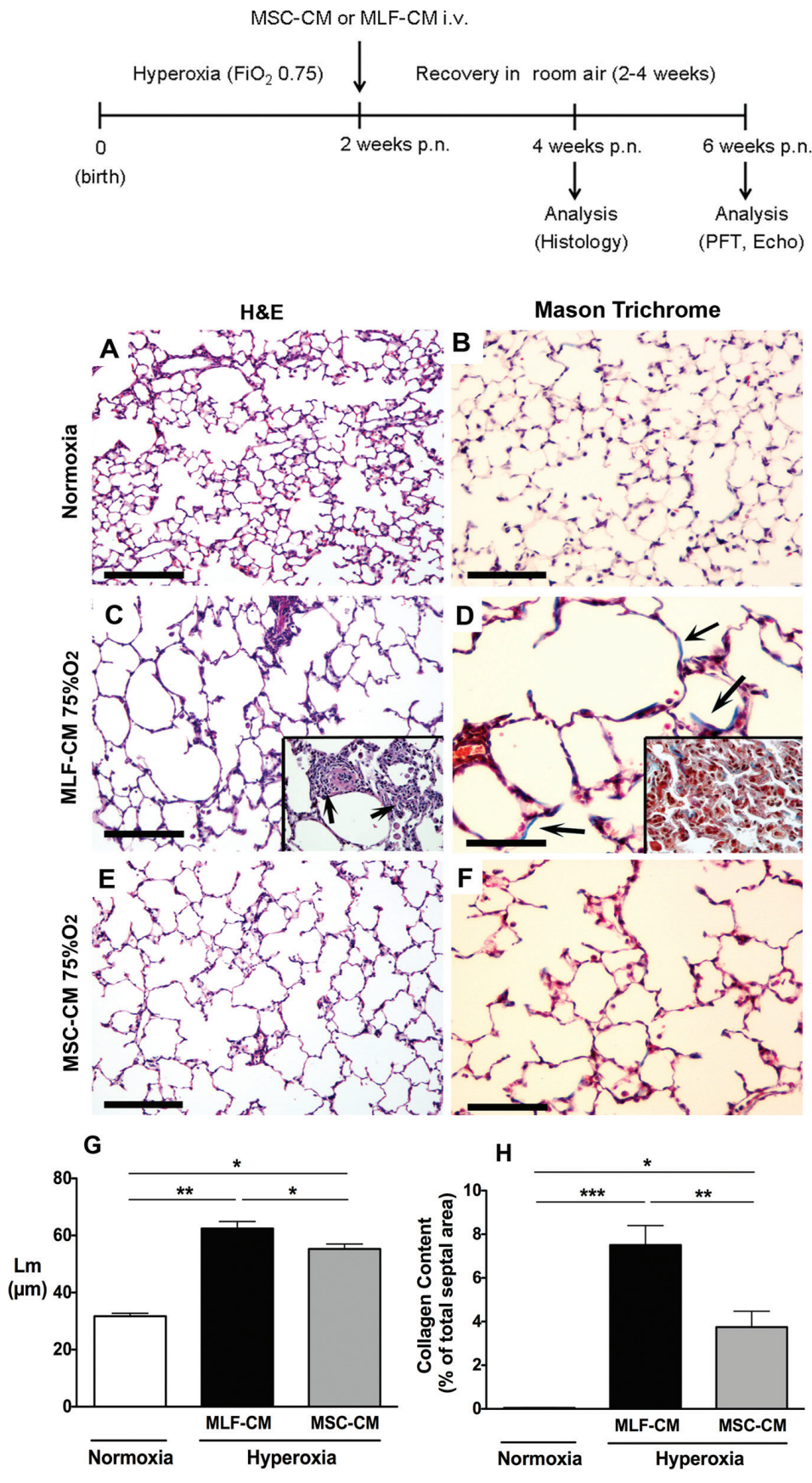


**Figure 1:** MSC-CM-treatment partially reverses neonatal hyperoxia-induced alveolar injury, septal thickening, collagen accumulation, myofibroblast infiltration, and inflammation. Upper panel: Experimental Design. Newborn mice were either left in room air, or exposed to hyperoxia (FiO<sub>2</sub>=0.75) for 2 weeks (P1-14), and then intravenously injected once with CM from either bone marrow-derived MSCs or primary MLFs, and placed in room air for 2 additional weeks, followed by harvest, inflation and fixation of lungs. Lung sections were stained for hematoxylin & eosin (A, C, E; 100×), and Mason Trichrome (B, D, F; 400×). Inserts were taken at 200× (H&E) and 400× (Mason Trichrome) magnification to illustrate interstitial inflammation (C, arrows), inflammation and fibrosis (D). Severe destruction of the alveolar architecture with overall widened airspaces and interstitial infiltration of inflammatory cells (macrophages, leukocytes) and myofibroblasts was seen in the hyperoxia-exposed/MLF-CM-treated mice (C, D) when compared to normoxic controls (A, B). Enhanced collagen deposition was seen in myofibroblasts, alveolar septa, and perivascular spaces in hyperoxia-exposed/MLF-CM-treated mouse lungs (D, arrows and inset). These changes were absent or greatly abrogated in MSC-CM-treated mice that had honeycomb-like alveoli (E, F) similar to normoxic controls, with residual emphysema. Quantification of mean linear intercept (Lm) as a surrogate of average air space diameter (G) and collagen content (H) are shown in the lower panels. Mean±SEM, n=4-7 per group, \*\*\*P<0.001, \*\*P<0.01, \*P<0.05. Scale bar = 100 μm (A, C, E) and 50 μm (B, D, F).



layered on a Ficoll-Paque (Amersham, Piscataway, N. J.) density gradient, centrifuged, and plated. Plastic adherent cells were maintained in culture with  $\alpha$ -MEM changed every two to three days. Following two to three passages, immunodepletion was performed as per published protocols and the International Society for Cellular Therapy (ISCT) guidelines.<sup>[26]</sup> The cells were negatively selected for CD11b, CD14, CD19, CD31, CD34, and CD45, and CD79 $\alpha$  antigens using the appropriate fluorescent-tagged antibodies (BD Biosciences, Pharmingen, San Diego, Calif.) in a fluorescence-activated cell sorter (MoFlo, Beckman-Coulter), further propagated, and then positively selected for CD73, CD90, CD105, c-kit, and Sca-1 antigens, as described. The differentiation potential of MSC cultures was assessed following published protocols.<sup>[26,27]</sup> Primary MLFs were derived according to the standard methods.<sup>[29]</sup>

### Preparation of mesenchymal stem cell-conditioned media

Bone marrow-derived MSC confluent cultures were incubated in serum-free  $\alpha$ -MEM media for 24 hours and the CM from equal numbers of cells in each culture were concentrated 10-fold using an Amicon Ultra Centrifugal Filter Device (Millipore Corporation, Billerica, Mass.) with a molecular weight cut-off of 10 kDa. MLF-CM in the same concentration and volume served as control. Cells were used for derivation of conditioned media between passages 8-10.

### Intravenous injection of MSC- and MLF-conditioned media

A volume of 50  $\mu$ l of MSC- or MLF-derived CM concentrate, equivalent to a total of 10  $\mu$ g MSC-CM protein per mouse, was injected via the superficial temporal vein or the jugular vein on P14. Under these conditions, survival of injected pups was greater than 90%.

### Echocardiography

Anesthesia was induced with isoflurane 3% and continued at 1–2% to a goal heart rate of 350–450 bpm. Transthoracic echocardiography was performed in anesthetized mice (FiO<sub>2</sub> 1.0) using the Vevo 2100 machine (Visual Sonics, Toronto, Calif.) and a 40 MHz linear transducer with simultaneous ECG recording. In the anteriorly angulated left parasternal long axis view, PW Doppler was applied to measure the pulmonary artery acceleration time (PAAT) and the PA ejection time (PAET). A short PAAT or small PAAT/PAET ratio indicates high peak systolic PA pressure, as previously described and validated.<sup>[30,31]</sup> In the right parasternal long axis view, M-mode was applied to determine RV anterior (free) wall thickness (RVWT) using a virtual guideline across the RV free wall and RV cavity that cuts through the mitral valve annulus.

### Pulmonary function tests

To evaluate lung function, mice were anesthetized with 80 mg/kg pentobarbital sodium i.p. Following tracheostomy, mice were mechanically ventilated at a rate of 150 breaths/minute, a tidal volume of 10 ml/kg, and a positive end-expiratory pressure (PEEP) of 3 cmH<sub>2</sub>O with a computer-controlled small animal ventilator (Scireq, Montreal, Canada). To evaluate bronchial hyperresponsiveness, normal saline alone and escalating doses of inhaled methacholine (1.6, 5, 16, and 50 mg/ml) were aerosolized by using an ultrasonic nebulizer (Scireq, Montreal, Canada). Average airway resistance was calculated at baseline and maximal values were recorded after each dose of methacholine. In addition, dynamic lung compliance (C<sub>dyn</sub>) was determined at baseline and minimum values after each methacholine dose were recorded.

### Lung tissue perfusion and histology

Following terminal anesthesia with 240 mg/kg Avertin i.p., lungs were perfused with PBS through the right ventricle at a constant pressure of 25 cmH<sub>2</sub>O. Lungs were inflated to a fixed pressure of 15–20 cmH<sub>2</sub>O with 4% paraformaldehyde and postfixed overnight, subsequently processed, and paraffin embedded for sectioning.

### Immunohistochemical staining

Lung tissue sections were deparaffinized in xylene and rehydrated. Immunohistochemical analysis was performed by incubating with the indicated primary antibody at a dilution of 1:200 (von Willebrand factor, vWF; rabbit polyclonal anti human; Dako), 1:125 (alpha smooth muscle actin,  $\alpha$ -SMA; mouse monoclonal; Sigma) overnight at 4°C after 20 minutes of blocking at room temperature to reduce nonspecific binding. Endogenous peroxidase activity was inhibited with 0.3% H<sub>2</sub>O<sub>2</sub> in methanol (Sigma). Secondary antibodies and peroxidase staining was performed according to manufacturer's instructions (Vector laboratories, Burlingame, Calif.). Slides were counterstained with methyl green.

### Lung parenchymal and pulmonary vascular morphometry and quantification

Lung sections were stained by Hematoxylin & Eosin (H&E) and Mason Trichrome (collagen). Ten randomly selected areas from 5  $\mu$ m H&E stained lung sections were captured at 100 $\times$  (H&E) and 400 $\times$  (Mason Trichrome) magnification using a Nikon Eclipse 80i microscope. Calibrations for the images were done by acquiring standard micrometer images using the same magnification. Large airways and vessels were avoided for the lung morphometry. The air space chord length (Lm) was calculated using Metamorph image analysis software (Molecular Devices, Sunnyvale, Calif). The images were superimposed on a grid with parallel lines

spaced at 58  $\mu\text{m}$  intervals, and the mean length of each chord, defined as the distance between two sequential intersections of the alveolar surface with the test line, was measured. The alveolar septal thickness ( $\mu\text{m}$ ) was calculated by measuring the fiber breadth (area/length) using Metamorph software. Peripheral vascularization was determined by counting the number of vWF-positive vessels in 15 random images at 200 $\times$  magnification, stratified by diameter (<50 and 50–100  $\mu\text{m}$ ), using Metamorph software. The vessel wall thickness was assessed by measuring  $\alpha$ -SMA positive staining in vessels less than 100  $\mu\text{m}$  diameter in 10–15 sections captured at 400 $\times$  magnification. The wall thickness was measured using Metamorph software and compared between groups using the following equation: Medial thickness index =  $[(\text{area}_{\text{ext}} - \text{area}_{\text{int}})/\text{area}_{\text{ext}}]$ , where  $\text{area}_{\text{ext}}$  and  $\text{area}_{\text{int}}$  are the areas within the external and internal boundaries of the  $\alpha$ -SMA layer, respectively.

### Pulmonary artery barium injections

A subset of left lungs (approximately half) were barium-infused via PA-inserted tubing to label central and peripheral pulmonary arteries for micro-CT-imaging, as previously described.<sup>[32]</sup> Barium was prepared by mixing 50 g gelatin (Sigma), 400 ml barium powder in 550 ml water, and injected at 60–70°C into the main pulmonary artery.

### Computed tomography and 3D reconstruction of PA barium injected mouse lungs

The basic method of micro-CT in vitro imaging has been previously described.<sup>[32]</sup> For this study, a Micro CAT II CT (Siemens) and RVA software was used. Formalin-fixated left lungs were each placed in an empty 50 ml Falcon tube and centered in the scanner by creating anterior-posterior and lateral X-rays images. A field of view of 768 $\times$ 768 voxels (1 voxel = 0.023 mm) was chosen. The left lungs of six weeks old untreated normoxic mice, hyperoxia-exposed/ MSC-CM-treated, or hyperoxia-exposed/MLF-CM-treated mice were fully scanned ex vivo at 45  $\mu\text{m}$  resolution (binning = 2) and 512 views (62 kVp, 1200 ms single image acquisition time), followed by realtime 3D reconstruction. Subsequently, Amira 4.1 software was applied on the 3D images. Isosurface rendering at a threshold of 1000 arbitrary units and appropriate positioning allowed display of all lungs in anterior-posterior views with best demonstration of segmental and peripheral branching of the left pulmonary artery.

### Statistical analysis

All values were expressed as means $\pm$ SEM. Comparison between different groups was performed by one-way ANOVA followed by Tukey's multiple comparison test, or unpaired Student's t-test, using GraphPad Prism 5.0 software (GraphPad, La Jolla, Calif.). *P* values <0.05 were considered significant.

## RESULTS

### MSC-CM-treatment reverses alveolar injury, septal thickening, and myofibroblast infiltration associated with hyperoxia-induced lung injury

Newborn mice exposed to two weeks of hyperoxia followed by a single dose of non-MSC control conditioned media (MLF-CM) showed severe destruction of the alveolar architecture with overall widened airspaces, alveolar simplification, airway remodeling, and interstitial infiltration of inflammatory cells (macrophages, neutrophils) and myofibroblasts, when compared to normoxic mice at four weeks of age (Fig. 1A–F). In the MLF-CM-treated animals, the many myofibroblasts within the alveolar walls had a high collagen content and frequently dendritic extensions elongating along the destructed alveolar remnants thereby creating ellipsoid to round structures (Fig. 1C and D). Collagen deposition, that was practically absent in normoxic mice, was also seen in alveolar septal and perivascular spaces of hyperoxia-exposed/MLF-treated mouse lungs (Fig. 1D). These hallmarks of dysfunctional pulmonary regeneration and fibrosis after hyperoxia in MLF-CM-treated animals were absent or greatly ameliorated in MSC-CM-treated mouse lungs that had honeycomb-like alveoli similar to normoxic controls (Fig. 1E and F). To quantify the effect of MSC-CM on hyperoxia-induced lung damage, septal collagen content, alveolar septal thickening, and Lm, as an approximation of alveolar air space diameter, were determined. MSC-CM-treatment after two weeks of hyperoxia decreased the deposition of alveolar septal collagen by 50% when compared to the hyperoxia-exposed/MLF-CM-treated animals (3.75 $\pm$ 1.92 vs. 7.51 $\pm$ 0.89% collagen staining of total septal area; *P*<0.01; Fig. 1H). Alveolar septal thickness, a combined variable of interstitial edema, inflammation, and parenchymal fibrosis, was quantified by measuring the fiber breadth (area/length). Septal thickening was evident in hyperoxia-exposed/MLF-CM-treated neonatal mice versus normoxic controls (3.92 $\pm$ 0.07 vs. 3.36 $\pm$ 0.20  $\mu\text{m}$ ; *P*<0.05), and ameliorated in animals that were treated with a single dose of MSC-CM (3.636 $\pm$ 0.05  $\mu\text{m}$ ; Fig. 1E and F).

The mean alveolar chord length was approximated by Lm measurements and was found to be increased by 97% in hyperoxia-exposed/MLF-CM-treated mice when compared to normoxic controls (Lm 62.4 $\pm$ 2.5 vs. 31.7 $\pm$ 1.0  $\mu\text{m}$ ; *P*<0.01). Hyperoxia-exposed/ MSC-CM-treated mice had significantly smaller airspaces (Lm 55.3 $\pm$ 1.7  $\mu\text{m}$ ; *P*<0.01) than MLF-CM-treated animals, but moderate residual emphysema four weeks postnatally when compared with normoxic controls (*P*<0.01; Fig. 1G). Thus, a single intravenous dose of MSC-CM improved the alveolar simplification, inflammation, and fibrosis associated with hyperoxia-induced BPD resulting in

moderate residual alveolar emphysema but otherwise near-normal lung structure.

### MSC-CM improves lung function after hyperoxia-induced lung injury

To determine the functional impact of the histological findings, we performed pulmonary function testing in 6-week-old mice 4 weeks after the end of hyperoxia, and in age-matched normoxic mice. All animals were ventilated at a PEEP of 3 cm H<sub>2</sub>O. Airway resistance was measured at baseline and after serial methacholine doses in order to quantify bronchial hyperreactivity. At baseline, the airway resistance was not different between the three groups (Fig. 2A). Intriguingly, MSC-CM-treatment fully reversed the abnormal increase in airway resistance response from low to high intratracheal methacholine doses (5, 16, 50 mg/ml) seen in the MLF-CM group to levels not different from normoxic controls (Fig. 2A). At a dose of 50 mg/ml intratracheal methacholine, dynamic lung compliance was greatly decreased in the hyperoxia-exposed/MLF-CM-treated mice when compared to normoxic controls, but was normal in the hyperoxia-exposed/MLF-CM-treated animals (Fig. 2B). Thus, MLF-CM-injected mice exposed to high oxygen concentrations had severe airway hyperresponsiveness to inhaled methacholine, consistent with our histological observations of airway remodeling and myofibroblast infiltration (Fig. 1C and D). However, MSC-CM-treated mice had normal dynamic lung compliance, and normal airway resistance (bronchial reactivity) responses to methacholine (Fig. 2), consistent with the histological findings (Fig. 1E and F vs. 1C and D).

### MSC-CM-treatment reverse pulmonary hypertension and RV hypertrophy in hyperoxia-induced lung injury

To assess the effects of hyperoxia and MSC-CM on both RV mass and PA pressure, M-mode and PW-Doppler echocardiography were applied. Compared with normoxia (Fig. 3A), the PAAT and PAAT/PAET ratios (i.e., surrogates of mean PA pressure) were found to be decreased in hyperoxia-exposed/MLF-CM-treated animals (Fig. 3C), but improved to normoxic values in hyperoxia-exposed/MLF-CM-treated mice (Fig. 3E) (PAAT: 10.87±0.45 vs. 14.92±0.36 vs. 15.22±0.34 ms in normoxic mice,  $P<0.001$ ; PAAT/PAET ratio: 0.174±0.007 vs. 0.235±0.005 vs. 0.231±0.008 ms in normoxic mice,  $P<0.001$ ). In accordance with the reversal of PH after MSC-CM-treatment, we found thickening of the RV free wall (i.e., RVH) in the hyperoxia-exposed/MLF-CM-treated mice (Fig. 3D) that was normalized in the MSC-CM-treated animals (Fig. 3F) (RVWT: 0.354±0.008 vs. 0.259±0.016 vs. 0.235±0.013 mm in normoxic mice,  $P<0.01$ ). Thus, a single dose of MSC-CM reversed the moderate pulmonary hypertension and RV hypertrophy that was associated with hyperoxia-induced BPD (Fig. 3G and H).

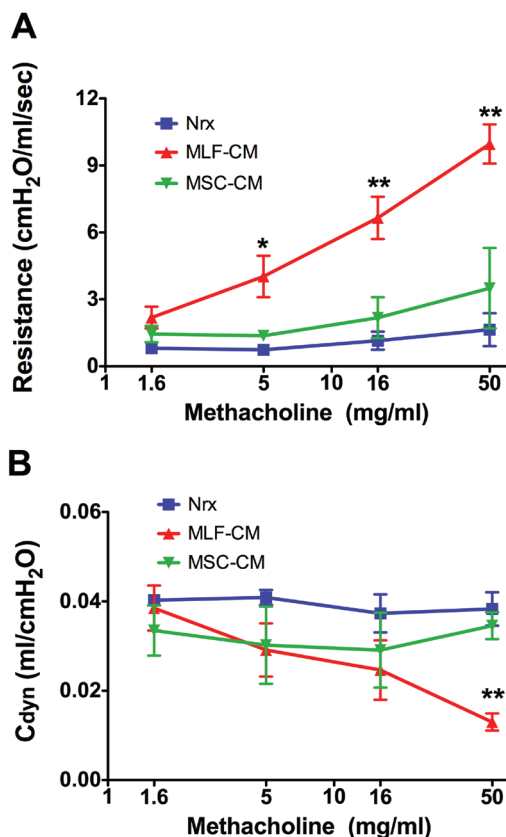


**Figure 2:** MSC-CM improve lung function after hyperoxia-induced lung injury. Pulmonary function testing was performed in six-week-old mice four weeks after the end of hyperoxia, and in age-matched normoxic control mice (see experimental design shown in Figure 1, and Methods section). Airway resistance (A) was measured at baseline and under escalating doses of intratracheal methacholine in order to quantify bronchial hyperreactivity. At baseline, airway resistance was not different between the three groups. MSC-CM-treatment fully reversed the abnormal increase in airway resistance seen in the MLF-CM group after administration of low to high intratracheal methacholine doses (5, 16, 50 mg/ml), to levels not different from normoxic controls (A). Dynamic lung compliance (C<sub>dyn</sub>) was remarkably impaired in the hyperoxia-exposed/MLF-CM-treated mice at a methacholine dose of 50 mg/ml but normal in the MSC-CM-treated mice when compared with normoxic controls, indicating normalized compliance under methacholine stress (B). The corresponding histological findings are shown in Figure 1. Mean±SEM, n=3–4 per group, \*\*  $P<0.01$ , \*  $P<0.05$ .

### MSC-CM attenuate hyperoxia-induced peripheral pulmonary arterial remodeling

To explore the potential impact of MSC-CM on hyperoxia-induced peripheral pulmonary vascular muscularization, random lung sections were stained for the smooth muscle marker,  $\alpha$ -SMA. The hyperoxia-induced enhancement of peripheral PA muscularization was already evident in the Mason Trichrome stained lung sections in the MLF-CM group (Fig. 1D) and confirmed by quantification of the SMA staining (Fig. 4). Accordingly, the medial thickness index was 46.3±1.8 versus 17.1±0.8 in normoxic controls ( $P<0.001$ ; Fig. 4B and D). A single dose of MSC-CM at the end of chronic hyperoxia ameliorated the abnormal peripheral PA muscularization seen in the



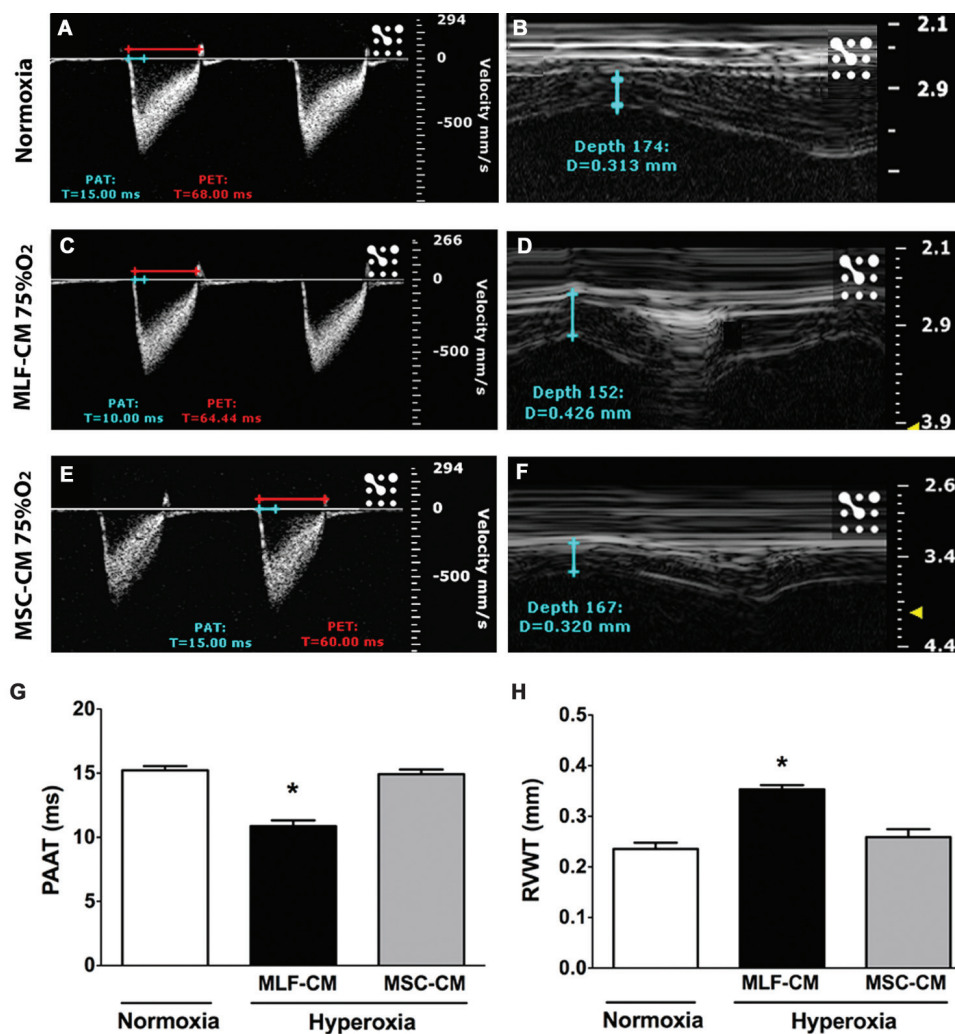


**Figure 3:** MSC-CM-treatment reverses pulmonary hypertension and RV hypertrophy in hyperoxia-induced lung injury. Pulmonary artery acceleration time (PAAT; syn. PAT), as a surrogate of mean PA pressure, was echocardiographically measured by PW-Doppler (A, C, E) and found to be shortened in hyperoxia-exposed/MLF-CM-treated animals (C), but normal in hyperoxia-exposed/MSC-CM-treated mice (blue line, E), when compared to normoxic controls (A, graphically summarized in G). Similar results were obtained for the PAAT/PAET ratio, where PAET is the pulmonary artery ejection time (syn. PET; data not shown). The end-diastolic diameter of the RV free wall (RVWT, RV wall thickness) was measured by M-mode echocardiography (B, D, F) and found to be increased in the hyperoxia-exposed/MLF-CM-treated mice but normalized in the MSC-CM-treated animals (H). Thus, a single dose of MSC-CM reversed the moderate pulmonary hypertension (G) and RV hypertrophy (H) that was associated with hyperoxia-induced BPD. See Figure 1 for experimental design. Mean±SEM, n=4 per group, \**P*<0.05.

MLF-CM-treated mice exposed to high inspiratory oxygen concentrations (medial thickness index  $40.8 \pm 1.7$ , *P*<0.05; Fig. 4C and D).

### MSC-CM rescue hyperoxia-induced loss of peripheral pulmonary blood vessels

In order to determine whether the loss of pulmonary vessels with chronic high oxygen exposure can be improved or reversed by a single dose of MSC-CM, quantification of pulmonary blood vessels of less than 50 and 50–100  $\mu$ m diameter was performed in vWF-stained lung sections. Hyperoxia led to significant loss of small vessels of less than 50  $\mu$ m diameter in the MLF-CM group (Fig. 5B and D), whereas MSC-CM injection restored the small (peripheral) vessels two weeks in recovery from chronic exposure to 75% oxygen (*P*<0.01; Fig. 5C and 5D). There was also a clear trend toward a protective effect of MSC-CM-treatment on the number of moderate-sized vessels (50–100  $\mu$ m) (MSC-CM vs. MLF-CM; *P*=0.0534; Fig. 5D). The counts of larger vessel were low and there was no significant difference in the quantity of vessels >100  $\mu$ m diameter between the groups (data not shown).

### MSC-CM reverse pulmonary artery pruning in hyperoxia-induced lung injury

To confirm the histological findings on the rescue of pulmonary vessel loss with MSC-CM-treatment, we performed PA barium injections and subsequent CT-3D reconstruction of the PA vascularization. In accordance with the histological evidence of peripheral vessel loss after chronic hyperoxia we found severe rarefaction of peripheral pulmonary arteries in lung CT scans of PA barium injected mouse lungs in the hyperoxia-exposed/MLF-CM-treated (control) group at four weeks recovery in room air (PA pruning; Fig. 6B). Hyperoxia-induced PA pruning was fully reversed by a single intravenous dose of MSC-CM given at the end of hyperoxia at P14, indicating a remarkable angiogenic/vasculogenic effect of MSC-CM (Fig. 6C).

## DISCUSSION

Chronic lung diseases such as BPD and pulmonary fibrosis will be the second leading cause of death

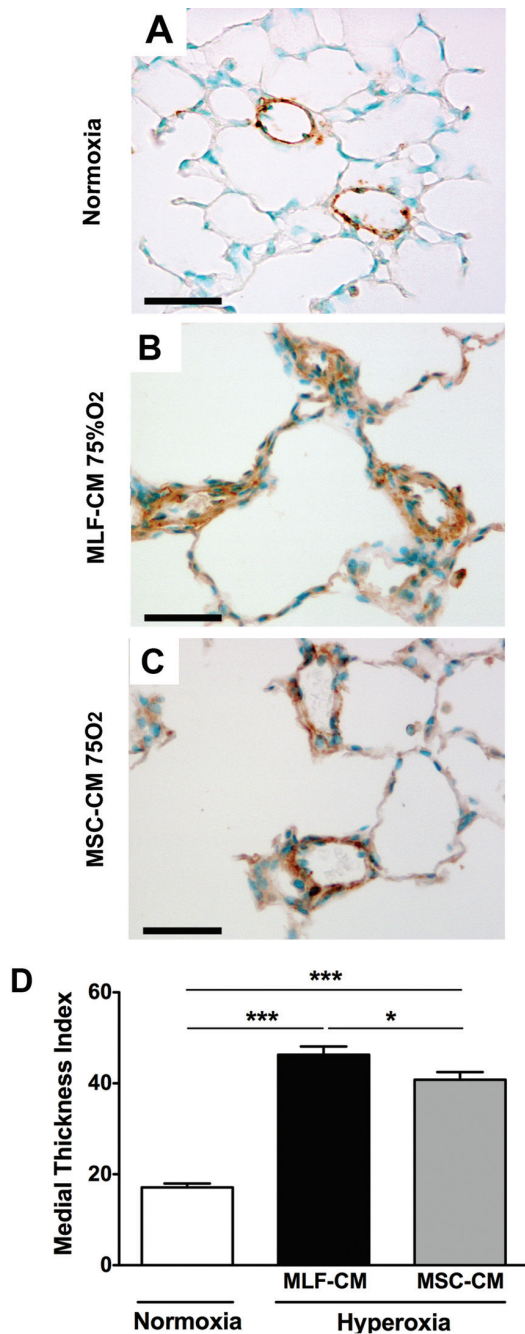


**Figure 4:** MSC-CM attenuate hyperoxia-induced peripheral pulmonary arteriole remodeling. Lung sections were stained for the smooth muscle marker,  $\alpha$ -SMA, and peripheral PA muscularization (<100  $\mu$ m outer diameter) quantified in random views at 400 $\times$  magnification as described under Methods. When compared to normoxic controls (A), hyperoxia exposure induced peripheral PA muscularization in the MLF-CM-treated mouse lungs (B) that was significantly reduced in the MSC-CM-treated lungs (C). Quantification of the  $\alpha$ -SMA staining is shown in D. See Figure 1 for experimental design. Mean $\pm$ SEM, n=4-7 per group, \*  $P$ <0.05. Scale bar=25  $\mu$ m.

worldwide by 2020.<sup>[33]</sup> BPD is a complex disease of premature infants with multiple pre and postnatal risk factors, including infection, preeclampsia, postnatal oxygen toxicity, and barotrauma, ultimately leading to

pulmonary inflammation and damage. Preterm infants are predominantly affected by the disease because of their underdeveloped airway supporting structures, surfactant deficiency, decreased lung compliance, and decreased antioxidant capacity. In the post-surfactant era, the pathobiology and clinical course of BPD has changed, and the disease is now characterized mainly by (1) impaired alveolarization with fewer, larger, and simplified alveoli, and (2) dysmorphic vasculogenesis, resulting in fewer (small) pulmonary arteries and frequently pulmonary hypertensive vascular disease that impacts survival. Additional features of the “new BPD” include inflammation, bronchial smooth muscle thickening, and interstitial edema.<sup>[1-4]</sup> Pulmonary hypertensive vascular disease in BPD is characterized by pulmonary arteriolar muscularization, vessel loss, and RV hypertrophy, among other findings.<sup>[2,7]</sup> Nearly all of these histological features – including excess myofibroblast proliferation and septal collagen deposition – were evident in the murine hyperoxia-BPD model used in this study.

To date, all available interventions for the prevention and/or treatment of BPD have not been effective in randomized controlled trials or have unacceptable adverse effects (e.g., postnatal glucocorticoids).<sup>[18]</sup> Prevention of premature birth and elimination of prenatal risk factors for BPD, such as preeclampsia<sup>[19,20]</sup> and chorioamnionitis,<sup>[21,22]</sup> is desirable but difficult to achieve. Therefore, finding an effective treatment approach for BPD and associated pulmonary vascular disease is of tremendous clinical importance.

There is emerging evidence from animal and clinical pilot studies that stem cell and progenitor cell-based therapies modulate disease markers and may be efficient in tissue/organ regeneration.<sup>[33,34]</sup> Bone marrow-derived MSCs have been shown to be efficient in the repair of heart and lung diseases such as myocardial infarction,<sup>[35]</sup> pulmonary fibrosis,<sup>[9]</sup> and LPS-induced lung injury.<sup>[9,36]</sup> Bone marrow-derived MSCs and MSC-CM from mice<sup>[11]</sup> and rats,<sup>[12]</sup> or human cord blood-derived MSCs,<sup>[37]</sup> when given intravenously or intratracheally in a preventive fashion, have been shown to improve lung architecture in rodent models of hyperoxia-induced BPD.

Previously, we demonstrated that intravenous injection of bone marrow-derived MSCs in newborn mice conferred significant vascular and immunological protection from hyperoxia-induced injury but had limited effect in preserving alveolar architecture.<sup>[11]</sup> Concentrated MSC-CM, however, prevented both vascular and alveolar hyperoxic injury resulting in normal alveolar number and thin septa, comparable to controls in room air.<sup>[11]</sup> The results of our previous preventive approach suggested that bone marrow-derived MSCs have important cytoprotective effects in the hyperoxia mouse model of developmental lung injury



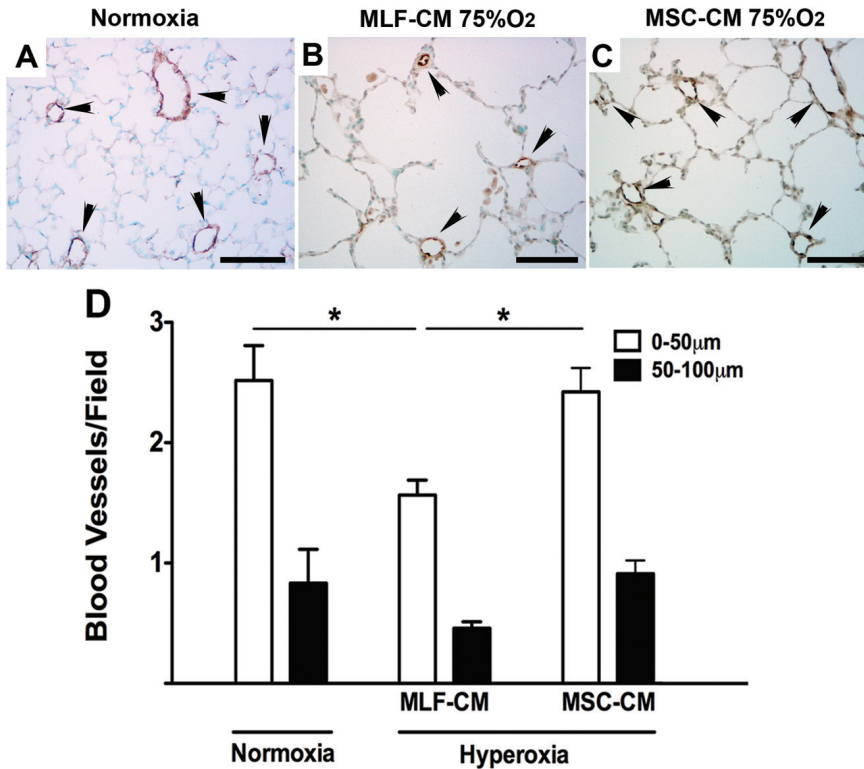


**Figure 5:** MSC-CM rescue hyperoxia-induced loss of peripheral pulmonary blood vessels. Lung sections were stained for the endothelial cell marker vWF. vWF-positive vessels between 25 and 200 μm outer diameter were counted at 200× magnification in 10–15 random views as described under Methods. Compared to normoxic controls (A), hyperoxia exposure led to significant loss of small vessels < 50 μm diameter in the MLF-CM group (B), whereas MSC-CM injection (C) restored small vessels after 2 weeks in recovery from chronic exposure to 75% oxygen (see Fig. 1 for experimental design). There was also a clear trend toward MSC-CM-treatment effect on the number of larger vessels (50–100 μm) in mice exposed to hyperoxia (MSC-CM vs. MLF-CM;  $P=0.0534$ ). Quantification of pulmonary blood vessels of less than 50 and 50–100 μm diameter in vWF-stained lung sections (D) was performed as described under Methods. There was no significant difference in numbers of larger vessels (100–200 μm) between the groups. See Figure 1 for experimental design. Mean±SEM,  $n=4-7$  per group, \*\*  $P<0.01$ , \*  $P<0.05$ . Scale bar = 50 μm.

mimicking BPD via paracrine mechanisms including the release of immunomodulatory and vasoprotective mediators.<sup>[11]</sup>

In the current study, we showed that a single intravenous dose of MSC-CM reversed – to a significant degree – hyperoxia-induced BPD and pulmonary vascular disease versus MLF-CM control: MSC-CM-treatment (1) reversed the hyperoxia-induced parenchymal fibrosis and peripheral PA devascularization (PA pruning), (2) partially reversed alveolar injury, (3) normalized lung function (airway hyperresponsiveness, dynamic lung compliance), (4) fully reversed the moderate PH and RVH, and (5) attenuated peripheral PA muscularization associated with hyperoxia-induced BPD.

The paracrine effects of MSCs include the release of immune and growth modulators identified in the CM by mass spectroscopy analysis.<sup>[11]</sup> These factors in MSC-CM promote signaling pathways of lung repair and include inhibitors of inflammation that are linked to the development of PH and pulmonary fibrosis. An attractive speculation is that the beneficial effect of MSC-CM may be, at least in part, due to activation of endogenous bronchioalveolar stem cells (BASCs), an adult lung stem cell population capable of self-renewal and differentiation in culture, and proliferation in response to bronchiolar and alveolar lung injury in vivo. Very recently, Tropea et al.<sup>[38]</sup> have demonstrated that intravenous treatment of neonatal hyperoxia-exposed mice with MSCs or MSC-CM led to a significant increase in

BASCs compared to untreated controls. Treatment of BASCs with MSC-CM in culture resulted in an increase in growth efficiency, suggesting a paracrine effect of MSCs on BASCs. Lineage tracing in bleomycin-treated adult mice showed that CCSP-expressing cells, including BASCs, are capable of contributing to alveolar repair after lung injury. Thus, MSCs and MSC-derived factors probably stimulate BASCs to contribute to the restoration of distal lung cell epithelia in BPD.<sup>[38]</sup>

Several studies have highlighted the existence of different MSC phenotypes in bone marrow, blood, and airways/lung. MSC phenotypes and function likely depend on maturity (gestational age) and environmental factors such as tissue oxygenation, and are distinctly regulated by the two major pathways of MSC differentiation, i.e., transforming growth factor beta (TGFβ) superfamily and canonical Wnt pathways.<sup>[35,39]</sup> Along these lines, in vitro treatment of airway MSCs of ventilated preterm infants with recombinant TGFβ1 induced myofibroblast differentiation, whereas adult human bone marrow-derived MSCs that were not exposed to high oxygen concentrations failed to undergo such differentiation upon TGFβ1 stimulation.<sup>[40]</sup> Popova et al. concluded that neonatal lung MSCs demonstrate an expression pattern characteristic of myofibroblastic progenitor cells (mRNAs encoding contractile and extracellular matrix proteins, and expression of α-SMA, MHC, and SM22 protein). Conditioned media from cultured tracheal aspirate MSCs of preterm infants exposed to hyperoxic stress contain

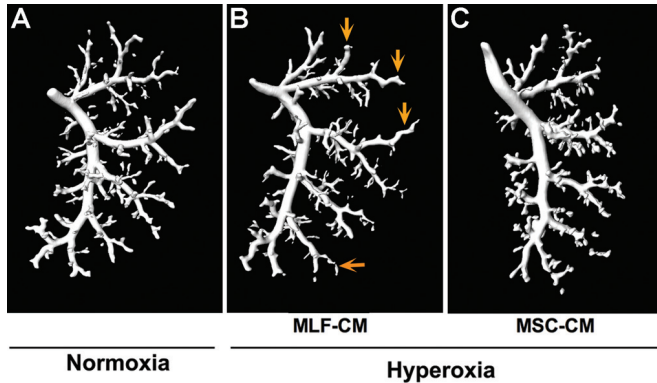


**Figure 6:** MSC-CM reverse pulmonary artery pruning in hyperoxia-induced lung injury. Pulmonary artery barium injections and subsequent computed tomography angiograms with 3D reconstruction of the PA vasculature of left lungs were performed *ex vivo*, as described in the Methods section. When compared to normoxic controls (A), severe rarefaction (pruning) of peripheral PAs (arrows) was evident on CT-angiograms of hyperoxia-exposed/MLF-CM-treated mice at 4 weeks recovery in room air (B). Such hyperoxia-induced PA pruning was completely absent in lungs from mice at 4 weeks recovery in room air injected with a single intravenous dose of MSC-CM at the end of hyperoxia exposure (C). For experimental design, see Figure 1.

high protein concentrations of TGF $\beta$ 1, and it was proposed that autocrine production of TGF $\beta$ 1 by neonatal lung MSCs drives myofibroblast differentiation;<sup>[40]</sup> however, it is yet unclear whether increased TGF $\beta$ 1 signaling and subsequent MSC to myofibroblast transdifferentiation occurs as a direct response to hyperoxia in the human preterm lung.

Importantly, increased expression of TGF $\beta$ 1 and Wnt has been reported in whole lung tissue of neonatal mice with hyperoxia-induced BPD and is associated with fibrosis in BPD<sup>[41-43]</sup> and several other CLD models.<sup>[44-46]</sup> However, alveolar myofibroblasts are required for the formation of secondary septa during normal lung development, a process that is arrested in BPD, indicating that the timing and adequate regulation of MSC differentiation is crucial for normal lung development.

Besides the bone marrow, multipotent MSCs have been shown to reside in the perivascular compartment of many organs,<sup>[24]</sup> and arise from both small and large arteries<sup>[47,48]</sup> as well as capillaries.<sup>[24]</sup> It was proposed that the tracheal aspirate MSCs found in one study in preterm infants who later on develop BPD are derived from the perivascular tissue of pulmonary and bronchial arteries.<sup>[49]</sup>

We speculate that hyperoxia-induced TGF $\beta$ 1 expression and secretion from airway/perivascular MSCs and other lung cells switches the phenotype of pulmonary MSCs and other proliferative cells toward pathological myofibroblast transdifferentiation resulting in dysfunctional repair (alveolar collagen accumulation/fibrosis and simplification, airway and pulmonary vascular remodeling, inflammation), consistent with

our histological findings. The report by Popova et al.<sup>[40]</sup> suggests that adult bone marrow-derived MSCs may be rather resistant to profibrotic stimuli such as hyperoxia and TGF $\beta$ 1. Our study shows that bone marrow-derived MSCs secrete factors with antifibrotic, antimitogenic, and anti-inflammatory effects that may regulate signaling downstream of the TGF $\beta$  receptor and inhibit myofibroblastic transdifferentiation of neonatal lung MSCs and/or alveolar epithelial type II cells. This is supported by our previous analysis of the MSC secretome.<sup>[11]</sup>

Recent experimental and clinical data suggest that hyperoxia induces BPD in premature newborns by impairing the number and *in vivo* functionality of circulating (blood), lung, and bone marrow endothelial progenitor cells (EPCs).<sup>[50,51]</sup> The quantity of circulating EPCs is low at extremely low gestational ages and increases during gestation. Importantly, extremely preterm infants who display lower EPC numbers in blood at birth have an increased risk of developing BPD.<sup>[52]</sup> Differentiation, release from bone marrow, tissue migration, and the predominant actions of EPCs in peripheral tissues/organs might be regulated by MSCs through paracrine mechanisms, as recently shown for BASCs (see above). In particular, the macrophage-colony stimulating factor (M-CSF) and granulocyte-colony stimulating factor (G-CSF) accelerate neovascularization *in vivo*<sup>[53]</sup> and induce differentiation of bone marrow cells into endothelial progenitor cells *in vitro*.<sup>[54]</sup> Interestingly, macrophage-CSF has been shown to induce EPC release from the bone marrow into the circulation through the augmentation of vascular endothelial growth factor (VEGF) production in bone marrow cells, especially from myeloid lineage cells.<sup>[55]</sup> Given that BMSC-CM are enriched in M-CSF,<sup>[11]</sup> a possible mechanism underlying the therapeutic action of BMSC-CM treatment is the mobilization of EPCs in the recipient animals. The latter would result in augmented neovascularization and the negation of the hyperoxia-induced pruning.

Possible risks of stem cell therapy include the potential for tumor formation and fibrosis. Indeed, fibrocytes, a pool of circulating mesenchymal precursors which can differentiate into myofibroblasts, were reported to be recruited to the lung and contribute to fibrosis<sup>[56]</sup> as well as pulmonary adventitial remodeling in experimental PH.<sup>[57]</sup> The human bone marrow, umbilical cord (tissue, blood), or placenta might serve as a source for MSC/ MSC-CM and probably will be used clinically as rescue therapy for BPD and other CLD in the near future, when safety of such interventions can be confirmed and the mechanisms of the important paracrine effects of MSCs are better understood (BPD-MS Phase I trials are underway: NCT01207869, NCT01297205, under <http://clinicaltrials.gov>). In particular, in-depth MSC characterization (e.g., surface markers), the composition and properties of

MSC-CM, the immunological responses to autologous or allogeneic MSC transplantation, certain compounds of MSC-CM, and the best source and route of administration need to be explored more comprehensively.

This study shows that a single intravenous dose of bone marrow-derived MSC-conditioned media rescues hyperoxia-induced BPD by reversing lung parenchymal fibrosis, pulmonary hypertension, vessel loss (PA pruning), and RV hypertrophy, significantly decreasing alveolar injury, reversing airway hyperresponsiveness, and normalizing dynamic lung function long-term. While the mechanisms underlying the beneficial effects of MSC-conditioned media will need to be explored in subsequent studies, MSC-derived interventions appear to be a promising treatment option for BPD, pulmonary hypertension, and other chronic lung diseases, and should be investigated in future clinical trials.

## ACKNOWLEDGMENTS

We thank Xianlan Liu for her expert technical assistance with the mouse breeding and oxygen exposures, Sarah Gately for the preparation of the manuscript, and Pat Dunning and Erin Snay for their technical assistance with micro-CT.

## REFERENCES

1. Jobe AH, Bancalari E. Bronchopulmonary dysplasia. *Am J Respir Crit Care Med* 2001;163:1723-9.
2. Stenmark KR, Abman SH. Lung vascular development: implications for the pathogenesis of bronchopulmonary dysplasia. *Annu Rev Physiol* 2005;67:623-61.
3. Thebaud B, Abman SH. Bronchopulmonary dysplasia: Where have all the vessels gone? Roles of angiogenic growth factors in chronic lung disease. *Am J Respir Crit Care Med* 2007;175:978-85.
4. Baraldi E, Filippone M. Chronic lung disease after premature birth. *N Engl J Med* 2007;357:1946-55.
5. Kim DH, Kim HS, Choi CW, Kim EK, Kim BI, Choi JH. Risk factors for pulmonary artery hypertension in preterm infants with moderate or severe bronchopulmonary dysplasia. *Neonatology* 2012;101:40-6.
6. Khemani E, McElhinney DB, Rhein L, Andrade O, Lacro RV, Thomas KC, et al. Pulmonary artery hypertension in formerly premature infants with bronchopulmonary dysplasia: Clinical features and outcomes in the surfactant era. *Pediatrics* 2007;120:1260-9.
7. Cerro MJ, Abman S, Diaz G, Freudenthal AH, Freudenthal F, Harikrishnan S, et al. A consensus approach to the classification of pediatric pulmonary hypertensive vascular disease: Report from the PVRI Pediatric Taskforce, Panama 2011. *Pulm Circ* 2011;1:286-98.
8. Warner BB, Stuart LA, Papes RA, Wispe JR. Functional and pathological effects of prolonged hyperoxia in neonatal mice. *Am J Physiol* 1998;275:L110-L7.
9. Ortiz LA, Gambelli F, McBride C, Gaupp D, Baddoo M, Kaminski N, et al. Mesenchymal stem cell engraftment in lung is enhanced in response to bleomycin exposure and ameliorates its fibrotic effects. *Proc Natl Acad Sci U S A* 2003;100:8407-11.
10. Weiss DJ, Bertonecello I, Borok Z, Kim C, Panoskaltis-Mortari A, Reynolds S, et al. Stem cells and cell therapies in lung biology and lung diseases. *Proc Am Thorac Soc* 2011;8:223-72.
11. Aslam M, Baveja R, Liang OD, Fernandez-Gonzalez A, Lee C, Mitsialis SA, et al. Bone marrow stromal cells attenuate lung injury in a murine model of neonatal chronic lung disease. *Am J Respir Crit Care Med* 2009;180:1122-30.
12. van Haften T, Byrne R, Bonnet S, Rochefort GY, Akabutu J, Bouchentouf M, et al. Airway delivery of mesenchymal stem cells prevents arrested alveolar growth in neonatal lung injury in rats. *Am J Respir Crit Care Med* 2009;180:1131-42.
13. Gupta N, Su X, Popov B, Lee JW, Serikov V, Matthay MA. Intrapulmonary delivery of bone marrow-derived mesenchymal stem cells improves survival and attenuates endotoxin-induced acute lung injury in mice. *J Immunol* 2007;179:1855-63.
14. Mei SH, McCarter SD, Deng Y, Parker CH, Liles WC, Stewart DJ. Prevention of LPS-induced acute lung injury in mice by mesenchymal stem cells overexpressing angiopoietin 1. *PLoS Med* 2007;4:e269.
15. Saugstad OD. Resuscitation of newborn infants: From oxygen to room air. *Lancet* 2010;376:1970-1.
16. Ozdemir R, Erdeve O, Dizdar EA, Oguz SS, Uras N, Saygan S, et al. Clarithromycin in preventing bronchopulmonary dysplasia in Ureaplasma urealyticum-positive preterm infants. *Pediatrics* 2011;128:e1496-501.
17. Gopel W, Kribs A, Ziegler A, Laux R, Hoehn T, Wieg C, et al. Avoidance of mechanical ventilation by surfactant treatment of spontaneously breathing preterm infants (AMV): An open-label, randomised, controlled trial. *Lancet* 2011;378:1627-34.
18. Gien J, Kinsella JP. Pathogenesis and treatment of bronchopulmonary dysplasia. *Curr Opin Pediatr* 2011;23:305-13.
19. Hansan AR, Barnes CM, Folkman J, McElrath TF. Maternal preeclampsia predicts the development of bronchopulmonary dysplasia. *J Pediatr* 2010;156:532-6.
20. Tang JR, Karumanchi SA, Seedorf G, Markham N, Abman SH. Excess soluble vascular endothelial growth factor receptor-1 in amniotic fluid impairs lung growth in rats: Linking preeclampsia with bronchopulmonary dysplasia. *Am J Physiol Lung Cell Mol Physiol* 2012;302:L36-46.
21. Watterberg KL, Demers LM, Scott SM, Murphy S. Chorioamnionitis and early lung inflammation in infants in whom bronchopulmonary dysplasia develops. *Pediatrics* 1996;97:210-5.
22. Paananen R, Husa AK, Vuolteenaho R, Herva R, Kaukola T, Hallman M. Blood cytokines during the perinatal period in very preterm infants: Relationship of inflammatory response and bronchopulmonary dysplasia. *J Pediatr* 2009;154:39-43 e3.
23. Hansmann G. Neonatal resuscitation on air: It is time to turn down the oxygen tanks [corrected]. *Lancet* 2004;364:1293-4.
24. Crisan M, Yap S, Casteilla L, Chen CW, Corselli M, Park TS, et al. A perivascular origin for mesenchymal stem cells in multiple human organs. *Cell Stem Cell* 2008;3:301-13.
25. Mangi AA, Noiseux N, Kong D, He H, Rezvani M, Ingwall JS, et al. Mesenchymal stem cells modified with Akt prevent remodeling and restore performance of infarcted hearts. *Nat Med* 2003;9:1195-201.
26. Peister A, Mellad JA, Larson BL, Hall BM, Gibson LF, Prockop DJ. Adult stem cells from bone marrow (MSCs) isolated from different strains of inbred mice vary in surface epitopes, rates of proliferation, and differentiation potential. *Blood* 2004;103:1662-8.
27. Dobson KR, Reading L, Haberey M, Marine X, Scutt A. Centrifugal isolation of bone marrow from bone: An improved method for the recovery and quantitation of bone marrow osteoprogenitor cells from rat tibiae and femur. *Calcif Tissue Int* 1999;65:411-3.
28. Dominici M, Le Blanc K, Mueller I, Slaper-Cortenbach I, Marini F, Krause D, et al. Minimal criteria for defining multipotent mesenchymal stromal cells. The International Society for Cellular Therapy position statement. *Cytotherapy* 2006;8:315-7.
29. McGowan SE. Influences of endogenous and exogenous TGF-beta on elastin in rat lung fibroblasts and aortic smooth muscle cells. *Am J Physiol* 1992;263:L257-63.
30. Thibault HB, Kurtz B, Raheer MJ, Shaik RS, Waxman A, Derumeaux G, et al. Noninvasive assessment of murine pulmonary arterial pressure: Validation and application to models of pulmonary hypertension. *Circ Cardiovasc Imaging* 2010;3:157-63.
31. Urboniene D, Haber I, Fang YH, Thenappan T, Archer SL. Validation of high-resolution echocardiography and magnetic resonance imaging vs. high-fidelity catheterization in experimental pulmonary hypertension. *Am J Physiol Lung Cell Mol Physiol* 2010;299:L401-12.
32. Hansmann G, Wagner RA, Schellong S, Perez VA, Urashima T, Wang L, et al. Pulmonary arterial hypertension is linked to insulin resistance and reversed by peroxisome proliferator-activated receptor-gamma activation. *Circulation* 2007;115:1275-84.
33. Siniscalco D, Sullo N, Maione S, Rossi F, D'Agostino B. Stem cell therapy: The great promise in lung disease. *Ther Adv Respir Dis* 2008;2:173-7.
34. McQualter JL, Bertonecello I. Concise Review: Deconstructing the lung to reveal its regenerative potential. *Stem Cells* 2012;30:811-6.
35. Williams AR, Hare JM. Mesenchymal stem cells: Biology, pathophysiology, translational findings, and therapeutic implications for cardiac disease. *Circ Res* 2011;109:923-40.
36. Lee JW, Fang X, Krasnodembskaya A, Howard JP, Matthay MA. Concise



- review: Mesenchymal stem cells for acute lung injury: Role of paracrine soluble factors. *Stem Cells* 2011;29:913-9.
37. Chang YS, Oh W, Choi SJ, Sung DK, Kim SY, Choi EY, et al. Human umbilical cord blood-derived mesenchymal stem cells attenuate hyperoxia-induced lung injury in neonatal rats. *Cell Transplant* 2009;18:869-86.
  38. Tropea KA, Leder E, Aslam M, Lau AN, Raiser DM, Lee JH, et al. Bronchioalveolar stem cells increase after mesenchymal stromal cell treatment in a mouse model of bronchopulmonary dysplasia. *Am J Physiol Lung Cell Mol Physiol* 2012;302:L829-L837.
  39. Augello A, De Bari C. The regulation of differentiation in mesenchymal stem cells. *Hum Gene Ther* 2010;21:1226-38.
  40. Popova AP, Bozyk PD, Goldsmith AM, Linn MJ, Lei J, Bentley JK, et al. Autocrine production of TGF-beta1 promotes myofibroblastic differentiation of neonatal lung mesenchymal stem cells. *Am J Physiol Lung Cell Mol Physiol* 2010;298:L735-43.
  41. Dasgupta C, Sakurai R, Wang Y, Guo P, Ambalavanan N, Torday JS, et al. Hyperoxia-induced neonatal rat lung injury involves activation of TGF-beta and Wnt signaling and is protected by rosiglitazone. *Am J Physiol Lung Cell Mol Physiol* 2009;296:L1031-41.
  42. Kumarasamy A, Schmitt I, Nave AH, Reiss I, van der Horst I, Dony E, et al. Lysyl oxidase activity is dysregulated during impaired alveolarization of mouse and human lungs. *Am J Respir Crit Care Med* 2009;180:1239-52.
  43. Nakanishi H, Sugiura T, Streisand JB, Lonning SM, Roberts JD Jr. TGF-beta-neutralizing antibodies improve pulmonary alveologenesis and vasculogenesis in the injured newborn lung. *Am J Physiol Lung Cell Mol Physiol* 2007;293:L151-61.
  44. Konigshoff M, Kramer M, Balsara N, Wilhelm J, Amarie OV, Jahn A, et al. WNT1-inducible signaling protein-1 mediates pulmonary fibrosis in mice and is upregulated in humans with idiopathic pulmonary fibrosis. *J Clin Invest* 2009;119:772-87.
  45. Henderson WR Jr, Chi EY, Ye X, Nguyen C, Tien YT, Zhou B, et al. Inhibition of Wnt/beta-catenin/CREB binding protein (CBP) signaling reverses pulmonary fibrosis. *Proc Natl Acad Sci U S A* 2010;107:14309-14.
  46. Wynn TA. Integrating mechanisms of pulmonary fibrosis. *J Exp Med* 2011;208:1339-50.
  47. da Silva Meirelles L, Chagastelles PC, Nardi NB. Mesenchymal stem cells reside in virtually all post-natal organs and tissues. *J Cell Sci* 2006;119:2204-13.
  48. Zannettino AC, Paton S, Arthur A, Khor F, Itescu S, Gimble JM, et al. Multipotential human adipose-derived stromal stem cells exhibit a perivascular phenotype in vitro and in vivo. *J Cell Physiol* 2008;214:413-21.
  49. Popova AP, Bozyk PD, Bentley JK, Linn MJ, Goldsmith AM, Schumacher RE, et al. Isolation of tracheal aspirate mesenchymal stromal cells predicts bronchopulmonary dysplasia. *Pediatrics* 2010;126:e1127-33.
  50. Balasubramaniam V, Mervis CF, Maxey AM, Markham NE, Abman SH. Hyperoxia reduces bone marrow, circulating, and lung endothelial progenitor cells in the developing lung: implications for the pathogenesis of bronchopulmonary dysplasia. *Am J Physiol Lung Cell Mol Physiol* 2007;292:L1073-84.
  51. Baker CD, Ryan SL, Ingram DA, Seedorf GJ, Abman SH, Balasubramaniam V. Endothelial colony-forming cells from preterm infants are increased and more susceptible to hyperoxia. *Am J Respir Crit Care Med* 2009;180:454-61.
  52. Borghesi A, Massa M, Campanelli R, Bollani L, Tziialla C, Figar TA, et al. Circulating endothelial progenitor cells in preterm infants with bronchopulmonary dysplasia. *Am J Respir Crit Care Med* 2009;180:540-6.
  53. Minamino K, Adachi Y, Okigaki M, Ito H, Togawa Y, Fujita K, et al. Macrophage colony-stimulating factor (M-CSF), as well as granulocyte colony-stimulating factor (G-CSF), accelerates neovascularization. *Stem Cells* 2005;23:347-54.
  54. Zhang Y, Adachi Y, Iwasaki M, Minamino K, Suzuki Y, Nakano K, et al. G-CSF and/or M-CSF accelerate differentiation of bone marrow cells into endothelial progenitor cells in vitro. *Oncol Rep* 2006;15:1523-7.
  55. Nakano K, Adachi Y, Minamino K, Iwasaki M, Shigematsu A, Kiriyama N, et al. Mechanisms underlying acceleration of blood flow recovery in ischemic limbs by macrophage colony-stimulating factor. *Stem Cells* 2006;24:1274-9.
  56. Moore BB, Kolodick JE, Thannickal VJ, Cooke K, Moore TA, Hogaboam C, et al. CCR2-mediated recruitment of fibrocytes to the alveolar space after fibrotic injury. *Am J Pathol* 2005;166:675-84.
  57. Frid MG, Brunetti JA, Burke DL, Carpenter TC, Davie NJ, Reeves JT, et al. Hypoxia-induced pulmonary vascular remodeling requires recruitment of circulating mesenchymal precursors of a monocyte/macrophage lineage. *Am J Pathol* 2006;168:659-69.

**Source of Support:** Supported by National Heart Lung and Blood Institute (NHLBI) grants R01 HL055454 (S.K.), R01 HL085446 (S.K.), and P50 HL067669 (S.K. and S.A.M.). M.A. was supported by 5T32 HD007466-12 (S.K., PI). **Conflict of Interest:** None declared.